

Alpeshbharathi R.
Gauswami^{1,2},
Hardik A. Shah³,
Shaktisinh N. Gohil⁴

Designing & Analyzing an EV Battery Charger with Enhanced Power Quality



Abstract: - The typical two-stage battery charger for Electric Vehicles (EVs) usually includes a front-end rectifier-powered switch mode power supply (SMPS). When EVs are connected to the utility grid, they cause harmonic currents in the AC lines. The presence of harmonics leads to voltage distortion, heating, and noise, ultimately diminishing the line's capacity. The design of a battery charger for an EV must aim to alleviate stress on the utility grid by minimizing total harmonic distortion (THD). Incorporating active power factor correction (PFC) with the front-end converter serves to lessen the phase difference between input current and voltage, and also decreases line current harmonics to comply with the specified IEC 61000-3-2 power quality (PQ) standard for EV battery chargers. This study entails the design and analysis of an EV battery charger with PFC. The simulation model of the EV battery charger is created using MATLAB Simulation software. The paper's discussion of design and analysis provides guidance for enhancing the performance of an EV battery charger with a PFC regulator.

Keywords: electric vehicle (EV), switch mode power supply (SMPS), power factor correction (PFC), total-harmonic-distortion (THD), power quality (PQ), battery charger.

1. INTRODUCTION

The front-end converter and SMPS play a crucial role in the on-board charger system for electric vehicles powered by AC lines. The on-board charger must satisfy the power quality requirements for AC supply mains as specified in regulatory standards like IEC 61000-3-2 and IEEE Std. 519. [1-3] The use of power electronics converters in non-linear loads connected to AC lines can have a negative impact on the power quality of the AC mains. Uncontrolled rectifiers and SMPS used in battery chargers draw non-sinusoidal currents from the AC mains, leading to current distortion in the line. The implementation of Power Factor Correction (PFC) is essential to make the line current sinusoidal and enhance power quality. The use of passive or active PF correction (PFC) techniques can help reduce harmonic content. Passive approaches offer a simple and sturdy solution, but they have a higher density due to tuned LC filters. Additionally, passive filters may not respond adequately to variations in load PF. In contrast, active methods utilize power semiconductor switches along with passive elements to address the drawbacks of passive techniques and provide a more effective solution. [4-6] The active PFC techniques for single phase can be categorized as either the single-stage approach or the two-stage approach. The single-stage approach is suitable for low power applications, while the two-stage approach is more appropriate for medium to high power applications. Most on-board battery charging systems consist of two cascaded stages. As a result, the two-stage approach is well-suited for EV battery chargers, especially when dealing with relatively high-power ratings and when lithium ion batteries serve as the primary energy storage system. [7]

The fig.1 illustrates a simplified system block diagram of an on-board two-stage battery charger. [7,8]

¹Research Scholar, Gujarat Technological University, Ahmedabad, Gujarat India.

Email:- alpesh.gauswami27@gmail.com

^{2,4}Assistant Professor, Power Electronics Department, Lukhdhirji Engineering College-Morbi, Gujarat India.

Associate Professor, Electrical Engineering, A.D.Patel Institute of Technology,
The Charutar Vidya Mandal (CVM) University, Vallabh Vidyanagar, Gujarat, India.

Corresponding Author: ee.hardik.shah@adit.ac.in

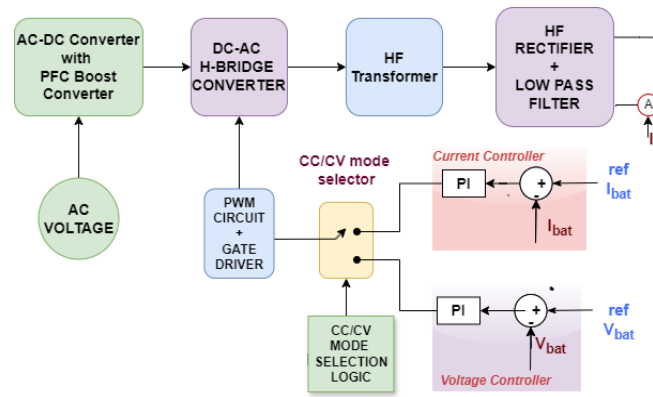


Fig.1 Simplified system block diagram of on-board two-stage battery charger

The uncontrolled converter converts the input AC voltage to a regulated intermediate DC link voltage by rectifying it. A DC-DC converter adjusts the output voltage based on the load requirements. The presence of nonlinear and storage elements can lead to undesirable effects such as input current waveform distortion and displacement between the angle of input voltage and current waveform, resulting in poor power factor. [9,10] Moreover, the input current takes the form of narrow pulses, leading to an increase in its RMS value. [11,12] The paper utilizes a full bridge topology of SMPS as a DC-DC converter. This regulated dc output voltage high power fixed-frequency converter offers step-up/down operation and provides galvanic isolation between input and output. [13,14]

A two stage EV charger for 1kW operation is implemented in this work. The detailed design, operation and performance are discussed and validate through MATLAB. [15] The advantage of the unidirectional PFC boost converter and full bridge DC-DC converter's simple design is utilized here. A constant voltage constant current charging scheme is use for EV battery charging. The paper is divided into several sections. Section 2 presents the converter topology and description. In section 3, the design of circuit parameters is discussed, while section 4 covers the simulation results. A conclusion is drawn in Section 5.

2. Converter Topology and Description

The arrangement of the two-stage EV battery charger is depicted in Fig. 1, with the first stage consisting of an AC-DC converter with power factor correction (PFC), followed by the second stage comprising a full bridge DC-DC converter. [16,17] The front-end AC-DC converter receives a single 230V, 50Hz AC source. It produces pulsating DC voltage and transfers it to the DC link capacitor to eliminate ripples. Simultaneously, PFC is used to achieve power factor correction. The first stage's output is then transferred to the second stage. A full bridge DC-DC converter utilizes four identical power semiconductor switches on the primary side, which are switched at high frequency. Power transfer and galvanic isolation are achieved using a high frequency transformer. For achieving the desired low output voltage, a high-frequency step-down transformer is selected. Fast recovery diodes in a full-wave rectifier bridge are used to rectify the secondary output voltage. An LC low pass filter is used to smooth out the secondary rectifier output. The filtered DC output is given to the battery.

3. Design consideration of EV charger

In this section design and selection of various components of EV charger are carried out. Design of EV charger is divided into following subsections.

1. Calculation of battery voltage & battery capacity.
2. Selection of DC link voltage & DC link capacitor.
3. Design of full bridge DC-DC converter.

3.1. Calculation of battery voltage & battery capacity

In this section the no. of cells required for proposed battery and output capacity of charger are calculated from the manufacturer's datasheet. The design parameters for the proposed study are as below: As per requirement and simulation purpose 36Ah, 48V lithium ion battery is selected. From data sheet selected battery has following parameters. [18]

Table 1 Battery Parameters

Battery Parameters	Value
Battery Voltage (V_b)	48V
Battery Capacity	36Ah
Maximum Voltage of Cell (V_{max})	4.2V
Minimum Voltage of Cell (V_{min})	3V
Nominal Voltage of Cell (V_{nom})	3.7V

According to above data, output voltage and power rating of charger are calculated. No. of required cell in series for 56V battery are given by,

$$No. \text{ of cell in series}(C_n) = \frac{V_b}{V_{nom}} = 13 \quad (1)$$

Output Voltage of charger is given by,

$$V_o = C_n * V_{max} = 56V \quad (2)$$

Here Input current to the battery is assumed 15A at which battery will be charged, so output power of charger will be,

$$P_o = V_o * I_o = 1kW \quad (3)$$

Where,

P_o = output power of the charger

V_o =output voltage of the charger

I_o =output current of the charger

For above Power rating & current rating, most suitable topology of SMPS is Full bridge DC-DC converter. For following parameters design of Boost Converter and PSFB converter is carried out,

- Input Voltage ($V_{in(min)}$) :195 VAC
- Output Voltage (V_{out}) :56 V
- output current: 15 A
- Output Power ($P_{OUT (max)}$) :1kW
- Switching frequency (f_s) :50 KHz
- line frequency :50 Hz

3.2. Selection of DC link voltage & DC link capacitor

The DC link voltage for 1- ϕ EV charger is 375V. The maximum input current ($I_{in(max)}$) occurs at the minimum input line voltage ($V_{DC (min)}$) with the maximum output Power. The minimum DC link voltage in case of 1- ϕ EV charger is 275V.

$$V_{DC(min)} > \sqrt{2} * V_{ac(min)} > \sqrt{2} * 195 > 275V \quad (4)$$

Where, $V_{ac(min)}$ is the minimum AC Input Voltage

Assuming that the percentage of non-conducting period is minimal, the required output capacitance of rectifier can be calculated as Equation 5 shows:

$$C_{DC(link)} = \frac{2 * p_{in}}{\pi * V_{DC(min)} * \Delta V_{DC(min)} * f_{line}} = 1800\mu F \quad (5)$$

3.3. Design of full bridge DC-DC converter

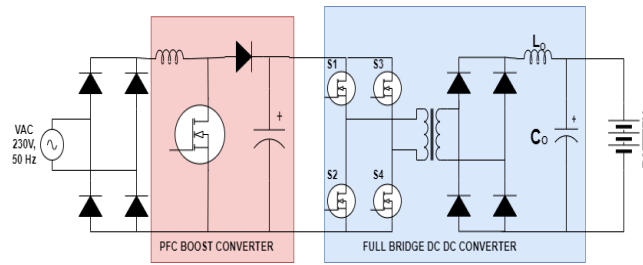


Fig.2 Schematic of proposed two-stage battery charger

3.3.1. Maximum “On” Time selection

In Figure.2, if two switches that are vertically arranged above one another (S2 and S1, or S3 and S4) are turned “on” simultaneously, they would present a dead short-circuit across the input and the semiconductor switch would fail. To protect switch, the maximum “on” time t_{on} will not be more than 80% of a half period. [19] The maximum “on” time occurs at minimum DC input voltage V_{dc} as can be seen in Equation 6.

$$V_o = V_{DC(min)} \times \frac{N_S}{N_P} \times 2 \times \frac{t_{on}}{T} \tag{6}$$

3.3.2. Transformer turns ratio

From equation 6 Transformer turn ratio n can be calculated as follows,

$$n = \frac{N_S}{N_P} = \frac{V_o}{2 \times V_{DC(min)} \times \frac{t_{on}}{T}} = 0.255 \tag{6}$$

Where,

t_{on} = maximum on time

T = Switching time

V_o = output voltage

$V_{DC(min)}$ = minimum input at FB converter

N_S = No. of turns for secondary

N_P = No. of turns for primary

3.3.3. Design of High frequency transformer

The process of designing a transformer begins by choosing a core that meets the required total output power. The power output available from a specific core relies on the frequency of operation, the density of the operating flux, the area of the core (A_e), the area of the bobbin winding window (A_b), and the current density in each winding. It is advisable to limit operation to within ± 1600 G even at frequencies up to approximately 50 kHz to prevent core saturation during transient conditions. [19] An initial estimation of the suitable core size is determined based on the core area product (A_p), which is calculated by the formula provided,

$$A_p = \frac{P_o \times D_{cma}}{0.0014 \times B_{max} \times f_s} = 3.75 \text{ cm}^4 \tag{7}$$

Where,

A_p = area product in cm^4

P_o = output power in watt

B_{max} = maximum flux density in gauss

f_s = switching frequency in hertz

D_{cma} = circular mils per RMS ampere

For above area product, ferrite Core (EE/56/28/21) is selected. For the EE/56/28/21 core, the area product can be obtained from the manufactures data sheet. For the of EE shape core the following core parameters are obtained [20].

- Effective volume :43900 mm³

- Effective length: 124 mm
- $A_e = 3.54 \text{ cm}^2$
- $A_w = 1.87 \text{ cm}^2$
- $A_p = 6.782 \text{ cm}^4$

3.3.4. Numbers of Primary turns and Numbers of Secondary turns

With a core selected and its iron area known, the number of primary turns is calculated at the the minimum primary voltage and the maximum “on” time of $0.8T/2$. [19,21]

$$N_p = \frac{(V_{dc}-1)(0.8T/2)}{A_e \times dB} \approx 20 \quad (8)$$

Secondary turns can be obtained using equation 9.

$$N_s = n \times N_p \approx 5 \quad (9)$$

3.3.5. Selection of wire size of transformer

Assume an efficiency of 80% from the primary input to the total output power. Then,

$$P_{in} = 1.25 \times P_o \approx 1050W \quad (10)$$

The equivalent primary flat-topped current I_{pft} is given by:

$$I_{pft} = \frac{1.56 \times P_o}{V_{dc}} = 3.36A \quad (11)$$

Primary Wire Size Selection

Current I_{pft} flows at a duty cycle of 0.8 so its RMS value is

$$I_{rms} = I_{pft} \times \sqrt{0.8} = 3A \quad (12)$$

At a current density of 500 circular mils per RMS ampere, the required number of circular mils is

$$\text{Circular mils needed} = \frac{500 \times 1.40 \times P_o}{V_{dc}} = 1507 \quad (13)$$

From the SWG table 18-gauge wire is used.

Secondary Wire Size Selection

RMS current in each half secondary is

$$I_{srms} = I_{dc} \times \sqrt{D} = 9.48A \quad (14)$$

At 500 circular mils per rms ampere, the required number of circular mils for each half secondary is

$$\text{Circular mils needed} = 500 \times I_{srms} = 4743 \quad (15)$$

3.3.6. Design of output filter

Design output filter inductor

$$L_o = \frac{(0.5-D) \times V_o \times T}{\Delta I_L} = 373\mu H \quad (16)$$

Where,

$T = \text{switching time (1/fs)}$

$\Delta I_L = \text{Output current ripple}$

Design output filter capacitor

$$C_o = \frac{(D) \times I_o \times T}{\Delta V_o} = 214\mu F \quad (17)$$

Where,

$RF = \text{ripple factor}$

4. Simulation and Results

Using the design parameters shown in table 2, the proposed EV charger is simulated in MATLAB-Simulink. For schematic shown in fig.2, simulation is performed with Matlab Simulink and results are taken.

Table 2 Battery Parameters

Design Parameter	Value
Input AC Voltage (V)	230
Switching Frequency (kHz)	50
Maximum Duty Cycle	0.4
DC link capacitor(μF)	1800
Transformer Turns Ratio	3
Output Filter Inductor(μH)	373
Output Filter Capacitor(μF)	214

The PFC converter stage is linked to the diode rectifier and is regulated using a variable duty cycle control method that is based on current hysteresis control. In this control technique, the PFC boost converter's output DC link voltage (V_{dclink}) is monitored and then compared with a set-point voltage (400V) in order to produce an error signal. The error signal that is produced is used to drive the PI controller, creating a control signal. This signal is then multiplied by the absolute value of the input AC voltage to produce the current reference signal. The resulting current reference is then compared to the actual input AC current to generate the final control signal, which is then input into the hysteresis-based PWM generating block. The output PWM signal is subsequently supplied to the switch utilized in the PFC boost converter. [22-27] The fig.3 shows the input voltage, current, and DC link voltage. The hysteresis control method offers several benefits. Upon circuit activation, the input AC current quickly adjusts its phase to match the input AC voltage, thereby improving power factor and minimizing input current harmonic distortion. The output response stabilizes within two to three cycles of the supply voltage.

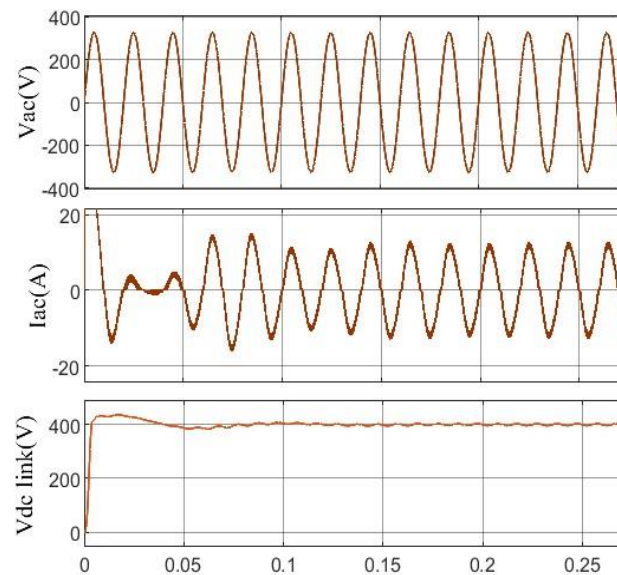


Fig.3 Input voltage (Vac), current (Iac) 1

The PFC stage decreases THD, enhances power factor, and also minimizes voltage and current fluctuations of the output DC voltage. As depicted in figure 3, the input ac current (I_{ac}) waveform is sinusoidal and synchronized with the input voltage (V_{ac}). The PFC stage transforms the unregulated output voltage of the diode rectifier into a stable DC voltage ($V_{dc-link}$) of 400V, which is then supplied to the DC/DC converter. DC link voltage obtained consists of small (<10%) double frequency voltage ripples. The total harmonics distortion (THD) is determined using FFT analysis tool available in the Simulink as shown in fig. 4. An THD of 6.94% is achieved, meeting the IEEE industrial standard- IEEE 519-2014 for AC supply.

The full bridge DC-DC converter is utilized to convert high voltage (400V) to a lower voltage ranging from 52-56V for the purpose of charging the battery. A constant voltage constant current charging method is employed for charging the lithium ion battery.

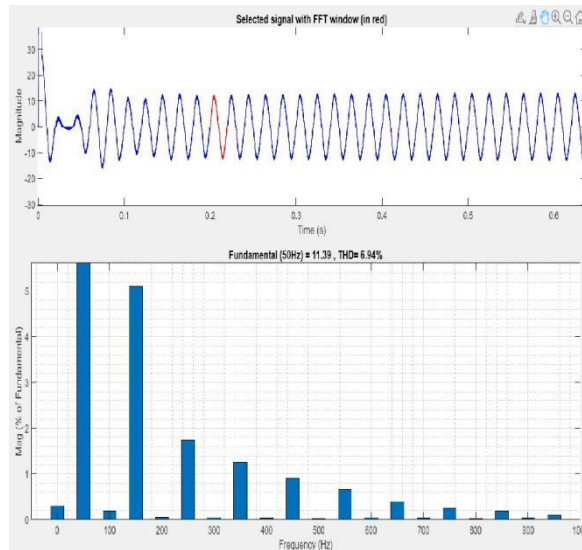


Fig.4 THD analysis result of input AC current

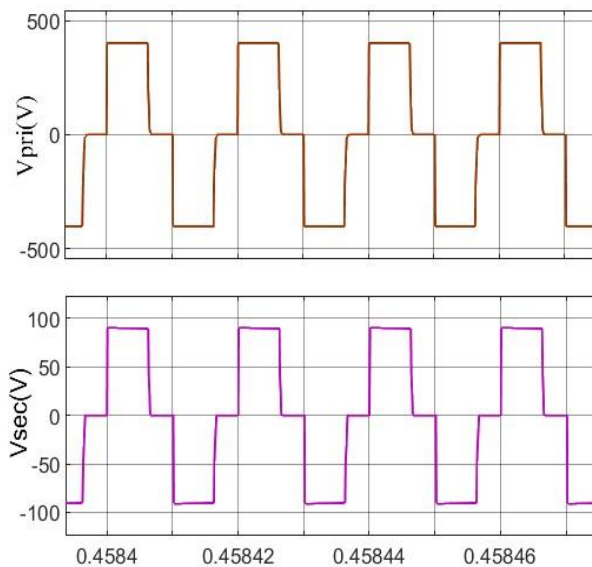


Fig.5 Voltage across primary winding, secondary winding

This control method involves the use of two PI controllers: one PI controller generates a control signal corresponding to the battery voltage, while the other generates a control signal corresponding to the battery current. Both PI controllers collaborate to produce the control signal. PWM signals and their complementary output signals, both operating at a frequency of 50kHz, are generated and applied to the four power switches of the full bridge DCDC converter. The resulting output voltage of the converter across the primary winding, secondary winding, and battery charging voltage is depicted in Fig.5.

Negative battery current implies that the battery is charging. When the battery is in steady state charging, the voltage is 55V and the current is 15A, resulting in a total output power of approximately 825W. The power supplied to the circuit is around 916W, resulting in an overall efficiency of 90%. Constant voltage mode is activated when the battery state of charge (SoC) reaches 80.05%. In constant voltage mode, the battery current decreases, leading to a longer charging time in hours to reach the remaining 20% SoC.

Lithium ion battery model of rating 48V/36AH is used as main load of the circuit. Initially battery SoC is set to 80%, the battery voltage and SoC increases gradually and current remains constant, in constant current mode as depicted in fig.6.

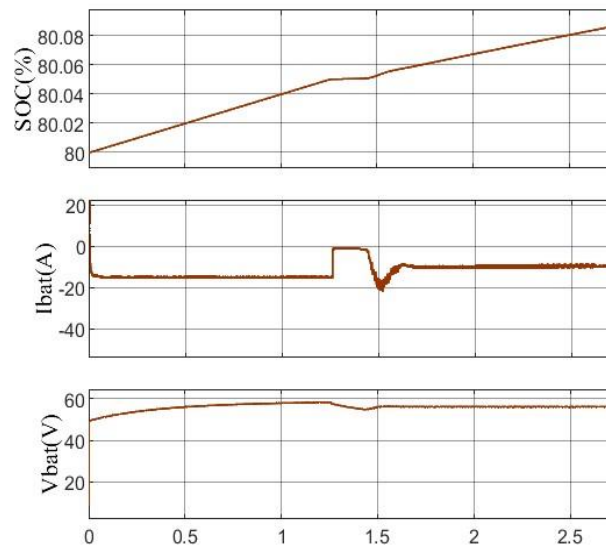


Fig.6 Battery SoC, current and voltage.

5. Conclusion

This paper provides a detailed analysis and simulation results of a battery charger system utilizing a PFC boost converter and a full-bridge DC-DC converter. The PFC boost converter enhances power factor to nearly unity, decreases THD to 6.94%, and minimizes voltage and current ripples of the DC-link voltage. Control of the PFC stage is achieved using the hysteresis current control method, while the full-bridge converter is managed by PWM signals. This converter transforms high input DC voltage (400V) into a lower voltage to charge a 48V lithium-ion battery. Lastly, a constant voltage constant current control algorithm is integrated for the full-bridge DC-DC converter. The system is specifically engineered to produce around 1kW of output power and demonstrates an efficiency of 90%. It is capable of charging e-bikes and e-autos equipped with 48V lithium-ion batteries.

REFERENCES

- [1] "Limits for Harmonics Current Emissions (Equipment current 16A per Phase)," *International standards IEC 61000-3-2*, 2000.
- [2] "IEEE recommended practices and requirements for harmonic control in electrical power systems," *IEEE Std 519-1992*, pp. 1–112, 1993.
- [3] "IEEE recommended practice and requirements for harmonic control in electric power systems," *IEEE Std 519-2014 (Revision of IEEE Std 519-1992)*, pp. 1–29, 2014. [<https://doi.org/10.1109/IEEESTD.2014.6826459>]
- [4] Rashid, M., Afridi, K., da Silva, J., Dillard, W., Dixon, J., Espinoza, J., Giesselmann, M., Hopkins, D., Khan, I., Krein, P., et al, "Power Electronics Handbook: Devices, Circuits and Applications," *Elsevier Science*, 2010. [<https://books.google.co.in/books?id=41-7BMFjnnnC>]
- [5] Potočny', M., Stopjakova', V., Kovač', M., "Design and verification of a low power ac/dc converter," *Journal of Electrical Engineering*, vol.72, no.2, pp.113–118, 2021. [<https://doi.org/doi:10.2478/jee-2021-0015>]
- [6] Shaktisinh Gohil, Hardik A. Shah, Utkal Mehta, "Comparing Various DC-DC Converters for Recharging EV Batteries," *Proceedings of International Conference on Computational Intelligence (ICCI 2023), Algorithms for Intelligent Systems (AIS)*, Springer, Singapore, ISBN 978-981-97-3526-6, pp. 101-115, 2024. [https://doi.org/10.1007/978-981-97-3526-6_9]
- [7] Yilmaz, M., Krein, P, "Review of battery charger topologies, charging power levels, and infrastructure for plug-in electric and hybrid vehicles," *Power Electronics, IEEE Transactions*, pp.2151–2169, 2013. [<https://doi.org/10.1109/TPEL.2012.2212917>]
- [8] Ferdous, S.M., Asaduzzaman Shoeb, M., Shafiuallah, G., Moin Oninda, M.A, "Parallel resonant converter for battery charging application," *9th International Conference on Power and Energy Systems (ICPES)*, pp.1–6, 2019. [<https://doi.org/10.1109/ICPES47639.2019.9105578>]
- [9] Martinez, R., Enjeti, P, "A high-performance single-phase rectifier with input power factor correction," *IEEE Transactions on Power Electronics*, vol.11, no.2, pp.311–317, 1996. [<https://doi.org/10.1109/63.486181>]
- [10] Schenk, K., Cuk, S, "A single-switch single-stage active power factor corrector with high quality input and output," *Record 28th Annual IEEE Power Electronics Specialists Conference. Formerly Power Conditioning Specialists Conference 1970-71*.

Power Processing and Electronic Specialists Conference 1972, vol. 1, pp. 385–391, 1997. [https://doi.org/10.1109/PESC.1997.616753]

- [11] Martinez, R., Enjeti, P, “A high-performance single-phase rectifier with input power factor correction,” *IEEE Transactions on Power Electronics*, vol.11, no.02, pp. 311–317, 1996. [https://doi.org/10.1109/63.486181]
- [12] Lalmalsawmi, Biswas, P.K, “Full-bridge dc-dc converter and boost dc-dc converter with resonant circuit for plug-in hybrid electric vehicles,” *International Conference on Intelligent Controller and Computing for Smart Power (ICICCSP)*, pp. 1–6, 2022. [https://doi.org/10.1109/ICICCSP53532.2022.9862426]
- [13] Wu, H., Xu, P., Hu, H., Zhou, Z., Xing, Y, “Multiport converters based on integration of full-bridge and bidirectional dc–dc topologies for renewable generation systems,” *IEEE Transactions on Industrial Electronics*, vol.61, no.02, pp.856–869, 2014. [https://doi.org/10.1109/TIE.2013.2254096]
- [14] Zhao, B., Song, Q., Liu, W., Sun, Y, “Dead-time effect of the high-frequency isolated bidirectional full-bridge dc–dc converter: Comprehensive theoretical analysis and experimental verification,” *IEEE Transactions on Power Electronics*, pp.1667–1680, 2014. [https://api.semanticscholar.org/CorpusID:22850476]
- [15] Inc., T.M, “Matlab version: 9.13.0 (r2018b),” 2018. [https://www.mathworks.com]
- [16] Nassary, M., Orabi, M., Ghoneima, M, “Discussion of single-stage isolated unidirectional ac-dc on-board battery charger for electric vehicle,” pp. 1–7, 2018. [https://doi.org/10.1109/SPEC.2018.8635919]
- [17] Prajapati, R., Naik, M.V, “Modelling and analysis of a pfc based ev battery charger using cuk-sepic converter,” *5th International Conference on Power, Control Embedded Systems (ICPCES)*, pp. 1–6, 2023. [https://doi.org/10.1109/ICPCES57104.2023.10075768]
- [18] LiTech Power Co.,Ltd, “Specification of LiTech Power Li-ion 20S12P 72V36Ah Battery Pack,” [https://www.litechpower.com/htmledit/uploadfiles/ /20220525032529697.pdf]
- [19] Pressman, A, “Switching Power Supply Design,” *McGraw-Hill*, 1998. [https:// books.google.co.in/books?id=txQJPlg4yZgC]
- [20] “E 55/28/21 Core and accessories. B66335, B66252, TDK Electronicsd,” 2022. [https://www.tdk-electronics.tdk.com/inf/80/db/fer/e_55_28_21.pdf]
- [21] Umanand, Z., Bhat, S, “Design of Magnetic Components For Switched Mode Power Converters,” *New Age International (P) Limited*, 1992. [https://books.google.co.in/books?id=gHBrPQAACAAJ]
- [22] Brahmabhatt, B., and H. Chandwani. "Modified second order generalized integrator-frequency locked loop grid synchronization for single phase grid tied system tuning and experimentation assessment." *International Journal of Engineering* 35.2 (2022): 283-290.
- [23] Kazerani, M., Ziogas, P., Joos, G, “A novel active current wave shaping technique for solid-state input power factor conditioners,” *IEEE Transactions on Industrial Electronics*, vol. 38, no. 1, pp. 72–78, 1991. [https://doi.org/10.1109/41.103488]
- [24] Brahmabhatt, Bhavik, and Hina Chandwani. "Single phase transformerless photovoltaic inverter with reactive power control." *2016 IEEE 1st International Conference on Power Electronics, Intelligent Control and Energy Systems (ICPEICES)*. IEEE, 2016.
- [25] Brahmabhatt, Bhavik, and Hina Chandwani. "Grid Synchronization for Three-Phase Grid-Tied Converter Using Decouple-Second-Order Generalized Integrator." *Proceedings of the International e-Conference on Intelligent Systems and Signal Processing: e-ISSP 2020*. Springer Singapore, 2022.
- [26] Borgonovo, D., Remor, J.P., Perin, A., Barbi, I, “A self-controlled power factor correction single-phase boost pre-regulator,” *IEEE 36th Power Electronics Specialists Conference*, pp. 2351–2357, 2005.
- [27] Kwon, J.M., Choi, W.Y., Kwon, B.H, “Cost-effective boost converter with reverse recovery reduction and power factor correction,” *IEEE Transactions on Industrial Electronics*, vol. 55, no. 1, pp. 471–473, 2008.